

## Research



**Cite this article:** Mohan JA, Miller NR, Herzka SZ, Sosa-Nishizaki O, Kohin S, Dewar H, Kinney M, Snodgrass O, Wells RJD. 2018 Elements of time and place: manganese and barium in shark vertebrae reflect age and upwelling histories. *Proc. R. Soc. B* **285**: 20181760. <http://dx.doi.org/10.1098/rspb.2018.1760>

Received: 3 August 2018

Accepted: 19 October 2018

**Subject Category:**

Ecology

**Subject Areas:**

ecology, biochemistry

**Keywords:**

shark, vertebral chemistry, barium, manganese, age, upwelling

**Author for correspondence:**

John A. Mohan

e-mail: [jmohan@tamu.edu](mailto:jmohan@tamu.edu)

Electronic supplementary material is available online at <https://doi.org/10.6084/m9.figshare.c.4280105>.

# Elements of time and place: manganese and barium in shark vertebrae reflect age and upwelling histories

John A. Mohan<sup>1</sup>, Nathan R. Miller<sup>2</sup>, Sharon Z. Herzka<sup>3</sup>, Oscar Sosa-Nishizaki<sup>3</sup>, Suzanne Kohin<sup>4</sup>, Heidi Dewar<sup>4</sup>, Michael Kinney<sup>5</sup>, Owyn Snodgrass<sup>5</sup> and R. J. David Wells<sup>1,6</sup>

<sup>1</sup>Department of Marine Biology, Texas A&M University at Galveston, 1001 Texas Clipper Road, Galveston, TX 77553, USA

<sup>2</sup>Jackson School of Geosciences, The University of Texas at Austin, 2275 Speedway Stop C9000, Austin, TX 78712, USA

<sup>3</sup>Departamento de Oceanografía Biológica, Centro de Investigación Científica y de Educación Superior de Ensenada (CICESE), 3918 Carretera Tijuana –Ensenada, Ensenada, Baja California 22860, Mexico

<sup>4</sup>Southwest Fisheries Science Center, and <sup>5</sup>Ocean Associates, Southwest Fisheries Science Center, National Marine Fisheries Service, 8901 La Jolla Shores Dr, La Jolla, CA 92037, USA

<sup>6</sup>Department of Wildlife and Fisheries Sciences, Texas A&M University, College Station, TX 77843, USA

JAM, 0000-0002-2758-163X; NRM, 0000-0002-1677-5594; SZH, 0000-0001-7091-7656; RJDW, 0000-0002-1306-0614

As upper-level predators, sharks are important for maintaining marine food web structure, but populations are threatened by fishery exploitation. Sustainable management of shark populations requires improved understanding of migration patterns and population demographics, which has traditionally been sought through physical and/or electronic tagging studies. The application of natural tags such as elemental variations in mineralized band pairs of elasmobranch vertebrae cartilage could also reveal endogenous and exogenous processes experienced by sharks throughout their life histories. Here, elemental profiles were characterized in vertebrae encompassing complete life histories (birth-to-death) of shortfin mako (*Isurus oxyrinchus*), common thresher (*Alopias vulpinus*) and blue shark (*Prionace glauca*) of known tag and recapture locations in the eastern North Pacific Ocean. All sharks were injected with oxytetracycline at initial capture, released and subsequently recaptured, with individual liberty times ranging from 215 days to 6 years. Vertebral band pairs forming over the liberty intervals were verified by counting the number of band pairs deposited since the oxytetracycline band. Regular oscillations in vertebrae manganese (Mn) content corresponded well with the number of validated band pairs, suggesting that Mn variation could be used to age sharks. Increases in vertebrae barium concentration were correlated with times when individuals occupied areas with high coastal upwelling indices, the timing and spatial intensity of which varied from year to year. Interspecific relationships were probably influenced by behavioural differences in horizontal and vertical habitat use, feeding habits and thermoregulatory physiology. These results indicate that vertebral sclerochronology has the potential to advance our knowledge of elasmobranch life history including age and growth estimation and environmental reconstruction.

## 1. Background

Most elasmobranchs grow slowly, mature late, and have low fecundity and (normally) high longevity, in comparison with most exploited teleost species, all of which magnify the impact of fishing exploitation on their standing stocks [1]. For regional management and conservation of mobile species, it is essential to

understand population productivity [2], dynamics of migration patterns, site fidelity, natal homing and connectivity within and among populations [3]. Highly migratory sharks transit through multinational waters where regulation is complicated and sharks are incidentally caught as by-catch in commercial longline, trawl, purse seine fisheries targeting other species and targeted in recreational fisheries [4]. In international fisheries, they are often not reported in catch statistics [5]. In addition to reliable catch statistics, accurate age and growth parameter estimates are particularly critical variables in stock assessment models, which are used to assess shark population demographics and setting target exploitation rates [1,6]. Incorrect age estimates can lead to erroneous conclusions regarding growth rates and population size, with severe consequences for shark population conservation [6].

Elasmobranchs are the only vertebrate group with non-bone cartilage skeletons reinforced with apatite [7]. Vertebrae columns of elasmobranchs grow radially and consist of calcified cartilage, which deposits calcium phosphate appositionally on an organic matrix [8]. Variations in calcium phosphate deposition result in the radial accretion of 'band pairs' that are distinguishable by optical properties due to different ratios of organic matrix to mineral content [9]. For most elasmobranch species, during fast summer growth, wider organic-rich hypomineralized zones are formed, whereas during slow growth, narrow hypermineralized zones are deposited, forming a band pair [9,10]. If the periodicity of band pair deposition is known or validated, then band pair counts can reveal age, since there is no resorption or remodelling of vertebral cartilage [11,12]. Several methods have been used to determine band pair periodicity in various species of elasmobranchs, including tag-recapture, marginal edge analysis, bomb radiocarbon and chemical tagging with oxytetracycline (OTC) [13]. Some of the limitations of these validation methods include the small sample sizes of recaptured sharks and that bomb radiocarbon techniques require that sharks were alive in the 1950s and 1960s, during and post-atomic bomb testing [14]. In addition, overall, age and growth studies using hard parts remain challenged by the difficulties of consistently and objectively identifying band pairs, and obtaining adequate sample sizes across the species size and geographical range.

To advance studies into age and growth as well as movement dynamics, researchers have examined the chemical composition of vertebrae. Although several studies have explored elemental variations (e.g. Ca, P, Sr) in vertebrae as they relate to band pair deposition [15–20], different species vary in their band pair elemental patterns. An early study of vertebrae band pair strontium (Sr) (in dogfish *Squalus acanthias* [18]) suggested Sr concentration was related to temperature and growth rate. Incorporation of other elements, such as Ba [16,21] and U [16], in addition to Sr [18,20,22,23] also appear to be mediated by the environment. Thus, vertebral band pair chemistry can reflect the ambient water mass or environmental conditions that a shark inhabited [21]. This interpretation has been widely used to assess movements across salinity gradients over ontogeny [22,23], geographical origin [24] and population structure [25–27]. While such studies assume element concentrations in vertebrae reflect ambient concentrations, the accuracy and precision of these interpretations remain tentative because the biochemical mechanisms of vertebrae mineralization are unknown [7] and few controlled laboratory experiments have been conducted to evaluate uptake of dissolved elements from water into vertebrae

cartilage [21]. It is extremely difficult to conduct controlled causal experiments with large-bodied animals, but field studies using mark–recapture provide a viable alternative.

Accurate interpretation of elemental patterns requires validation studies, and no studies to date have explored elemental patterns in OTC age-validated sharks with known capture locations in natural conditions. Specimens for this study were provided from previous OTC age-validation studies of three federally managed shark species in the North Pacific Ocean's eastern boundary current, a highly productive system driven by coastal upwelling. The three species exhibit contrasting movement patterns: the shortfin mako *Isurus oxyrinchus*, which occupies coastal and oceanic habitats [28,29]; common threshers *Alopias vulpinus*, which primarily occupy coastal habitats [30] and blue sharks *Prionace glauca*, which are predominantly oceanic [31,32]. All three species interact with fisheries and are either targeted or taken incidentally. Effective management/stewardship of shark populations requires accurate sampling tools to improve understanding of migratory behaviour and population dynamics. This study explores chemical patterns in age-validated shark vertebrae with known capture–recapture locations, employing a natural based experiment to directly relate elemental variation to band pair deposition and environmental conditions in the southern California–Baja Mexico coastal upwelling ecosystem. The research objectives of this study were (1) to establish birth-to-death vertebral elemental profiles in species with contrasting movement patterns and habitat use and (2) to compare the documented vertebral elemental signatures with chemical oceanographic characteristics of tagging and recapture locations within the coastal upwelling system.

## 2. Methods

### (a) Shark tagging and recapture

Details of shark tagging with OTC and recapture can be found in [28,33] for shortfin mako, [34] for common thresher shark and [31] for blue shark. In brief, sharks were captured using a pelagic longline, brought onto a tagging cradle, and given an intraperitoneal injection of OTC at a dose of 25 mg kg<sup>-1</sup> body mass, tagged externally with dart/roto tags containing recapture information, and then released. All OTC tagging was conducted in the summer months (June–September) and recaptures occurred from the spring throughout the autumn (see electronic supplementary material, table S1). Shortfin mako were recaptured in both coastal and oceanic environments, common thresher were primarily recaptured in coastal habitats and blue shark were mostly recaptured in oceanic locations (figure 1). Vertebrae from 10 shortfin mako, 10 common thresher and six blue shark were included in this study (see electronic supplementary material, table S1). Time at liberty varied for each species, with shortfin mako ranging from 277 to 2196 d, common thresher ranging from 267 to 1385 d and blue shark ranging from 215 to 587 d. Only one adult shortfin mako, that was at liberty for 6 years, was included in the study (A039494 [33]); all other sharks were juveniles or sub-adults. Annual deposition of band pairs has been validated in common thresher [34,35] and blue shark [31]; however, shortfin mako exhibit bi-annual deposition of band pairs when young, but transition to single band pair deposition at an unknown age [33].

### (b) Vertebrae preparation and analysis

Vertebrae centra were either stored dry, frozen or in ethanol, as previous experiments have demonstrated minimal influence of

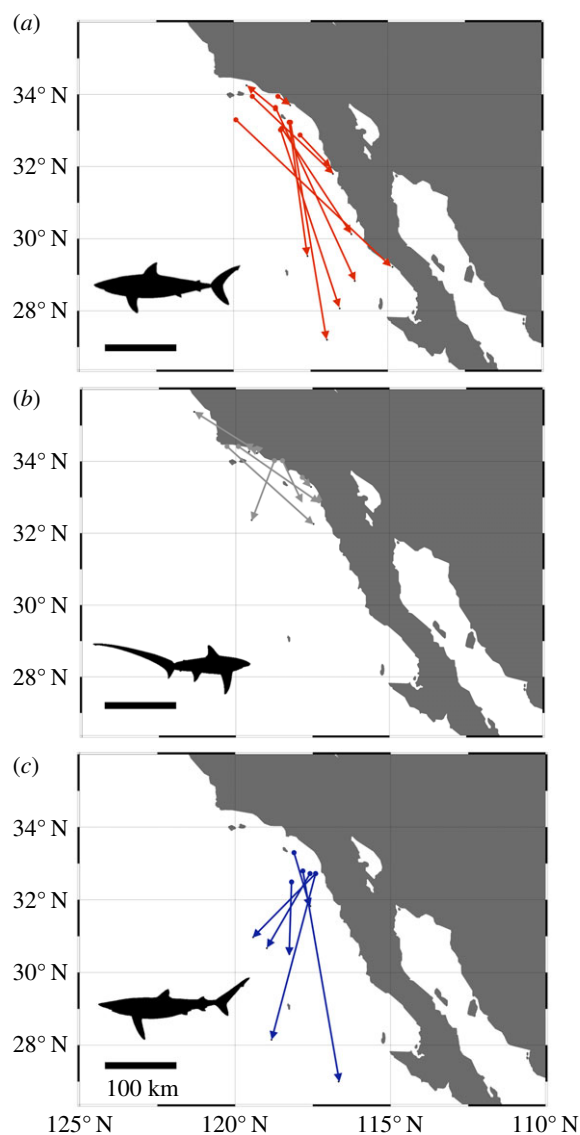


**Figure 1.** Map of shark capture and OTC tagging (circle) and recapture (arrow) locations for (a) shortfin mako (red), (b) common thresher (grey) and (c) blue sharks (blue) along the southern California coast, USA and the Baja California Peninsula, Mexico. See electronic supplementary material, table S1 for dates and duration between capture and recapture. (Online version in colour.)

these storage methods on primary elemental composition [36]. Vertebrae centra were cut using a low-speed diamond blade saw along central longitudinal planes to obtain approximately 2 mm thick central ‘bowtie’ sections. Sectioned ‘bowties’ were affixed to petrographic slides using thermoplastic cement (Crystalbond). Elemental concentrations in the direction of radial (outward) growth were quantified using a New Wave Research UP 193-FX fast excimer (193 nm wavelength, 4–6 ns pulse width) laser system coupled to an Agilent 7500ce inductively coupled mass spectrometer at the University of Texas at Austin. The laser system is equipped with a large format two-volume laser cell, which accommodated all shark vertebrae mounts and standards in a single loading with analysis occurring over 48 h. We first established a two-dimensional chemical map over a  $1.5 \times 4.5$  mm area of shortfin mako sample A038423 that encompassed the complete corpus calcareum, from the vertebral focus to the marginal edge. Analytical parameters were 90% laser power, 20 Hz repetition rate,  $15 \times 15 \mu\text{m}^2$  aperture,  $150 \mu\text{m s}^{-1}$  scan rate and a He cell flow of  $800 \text{ ml min}^{-1}$ . Prior to analysis, the sample was pre-ablated at 70% power, 20 Hz, using a  $150 \mu\text{m}$  spot scanning at  $150 \mu\text{m s}^{-1}$ . The imaged area involved 101 line traverses, spaced  $15 \mu\text{m}$  apart, with standards (NIST 612) analysed each hour. Single line transects

were completed for all other vertebrae samples. Laser ablation parameters optimized from test ablations were 60% laser power, 10 Hz repetition rate,  $100 \mu\text{m}$  spot,  $10 \mu\text{m s}^{-1}$  scan rate and a He cell flow of  $800 \text{ ml min}^{-1}$ . Prior to analysis, sample and standard traverses were pre-ablated at 60% power using a  $125 \mu\text{m}$  spot scanning at  $100 \mu\text{m s}^{-1}$ , to remove potential surface contamination. Laser transect analyses were bracketed every hour by standard measurements (USGS MAPS-4, MACS-3, and NIST 612; measured in triplicate for 60 s). Laser energy densities over the analytical sessions averaged  $3.07 \pm 0.08 \text{ J cm}^{-2}$  for line traverses. The quadrupole time-resolved method measured six masses using integration times of 10 ms ( $^{24}\text{Mg}$ ,  $^{43}\text{Ca}$ ,  $^{55}\text{Mn}$ ,  $^{88}\text{Sr}$ ) and 20 ms ( $^{66}\text{Zn}$ ,  $^{138}\text{Ba}$ ). Time-resolved intensities were converted to concentration (ppm) equivalents using Iolite software (Univ. Melbourne [37]), with  $^{43}\text{Ca}$  as the internal standard and a Ca index value of 35 weight % ([38], table III). Concentration (in ppm) was also expressed as molar ratios to calcium (in  $\mu\text{mol mol}^{-1}$ ), to make data units comparable to previous studies. Baselines were determined from 30 s gas blank intervals measured while the laser was off and all masses were scanned by the quadrupole. USGS MAPS-4 was used as the primary reference standard. Analyte recoveries for secondary standards MACS-3 and NIST 612, respectively, averaged  $106 \pm 1.1\%$  and  $112 \pm 0.1\%$  ( $n = 18$ ; versus GeOREM preferred values; <http://georem.mpch-mainz.gwdg.de>). Image data were processed using IOLITE [37]. Digital images of each vertebrae were acquired on a stereoscope mounted with a camera and measurements recorded in IMAGEJ software. Distance (in  $\mu\text{m}$ ) along each vertebrae were measured in triplicate and averaged for: (i) initial focal point ablation to birth band; (ii) from birth band to edge; (iii) from OTC mark to edge; and (iv) from focal point to edge of vertebrae. The elemental transect between the visible OTC mark and vertebrae outer edge, represents the capture–recapture migration time within the coastal region.

### (c) Data analysis

Elemental transect data were smoothed using 7-point median followed by 7-point moving average to remove high-frequency noise. To make comparisons of Mn : Ca data among species, concentration data were further smoothed using a second-order 50 nearest-neighbour smoothing function, and values were then expressed as a proportion of the maximum value in individual time series to normalize variable concentrations among species and plotted for each shark (see the electronic supplementary material, figure S1). Normalized Mn peaks were counted by three independent readers and reported as mean  $\pm$  s.e. Vertebral Ba : Ca concentrations were averaged across distances of  $100 \mu\text{m}$  at the OTC mark (known capture) and at the vertebrae edge (known recapture). The average daily accretion rate for all juvenile shark vertebrae was  $3.6 \pm 1.2 \mu\text{m d}^{-1}$  (electronic supplementary material, table S1); thus,  $100 \mu\text{m}$  of elemental data represents approximately one month (28 d) (electronic supplementary material, figure S1).

Coastal upwelling indices, which estimate the intensity of Ekman transport based on offshore wind measurements, were obtained from the Pacific Fisheries Environmental Laboratory website (<http://pfeg.noaa.gov/products/PFEL/modeled/indices/PFELindices.html>). Upwelling stations closest to the point of capture and recapture for individual shark specimens (specifically stations A:  $36^\circ \text{ N } 122^\circ \text{ W}$ ; B:  $33^\circ \text{ N } 119^\circ \text{ W}$ ; C:  $30^\circ \text{ N } 119^\circ \text{ W}$ ; and D:  $27^\circ \text{ N } 116^\circ \text{ W}$ ) were selected to obtain monthly upwelling indices. Upwelling indices for the month of capture and the previous month were summed, to account for lagged effects of upwelling on food webs and transfer of primary production across trophic levels. Linear regression analysis was performed to investigate how well band pair counts/validated age and upwelling indices (independent variables) predicted vertebral Mn : Ca and Ba : Ca (dependent variables), respectively.

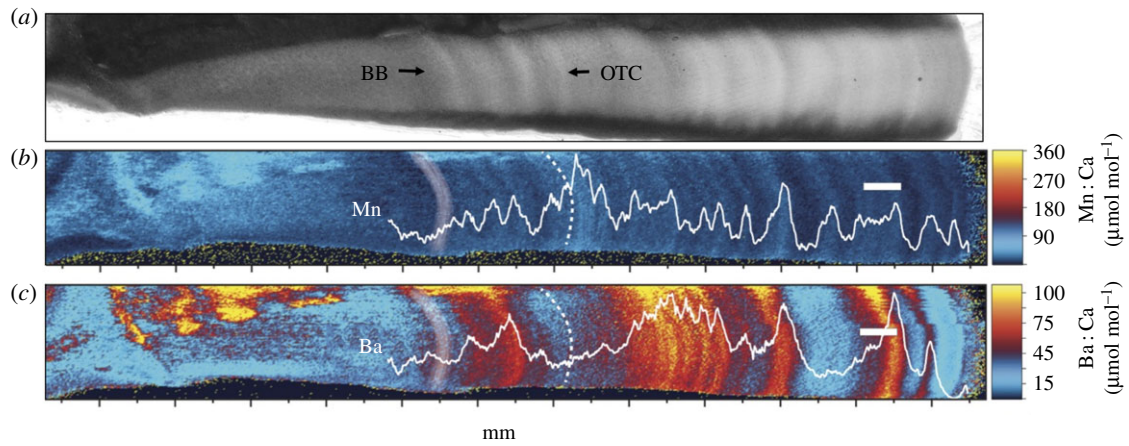


**Figure 2.** (a) Image of shortfin mako (ID: A038423) vertebrae under transmitted light, and (b,c) two-dimensional elemental map of (b) manganese and (c) barium variation. Birth band (BB) denoted in (b) and (c) with white shading and oxytetracycline band (OTC) denoted with dashed lines. Translucent zones (hypermineralized, slow growth) in a), matches with Mn decreases; opaque hypomineralized high protein zones matches with Mn peaks. White scale bar, 500  $\mu\text{m}$ .

### 3. Results

The two-dimensional elemental map of the single shortfin mako vertebrae corpus calcareum reveals that Mn and Ba concentrations oscillate between lower and higher concentrations, but at differing frequencies (figure 2). The other elements quantified did not exhibit consistent patterns and thus are not presented (but see electronic supplementary material, figure S2). The period of Mn spatial variation appears to correspond well with visible banding patterns (figure 2a,b). Barium patterns, however, are more variable, ranging from elevated values that span multiple years of growth, to lower values in other years (figure 2c). Comparison between the two-dimensional elemental map and a single laser transect along the centre of the corpus calcareum indicate that laser transects accurately track radial variability of Ba:Ca and Mn:Ca during vertebrae growth (figure 2), and that single transects sufficiently capture element patterns.

We next compared single laser transect profiles in Mn:Ca and Ba:Ca among individuals of other species. For Mn:Ca, we found that the number of smoothed and normalized post-OTC peaks consistently related to the number of band pairs and validated age for each species (figure 3). However, relationships were species-specific, with shortfin mako having  $1.08 \pm 0.16$  Mn peaks per band pair (figure 3a) and  $2.68 \pm 0.50$  Mn peaks  $\text{yr}^{-1}$  (figure 3d); common thresher having  $1.33 \pm 0.28$  Mn peaks per band pair (figure 3b) and  $1.63 \pm 0.17$  Mn peaks  $\text{yr}^{-1}$  (figure 3e); and blue shark having  $5.10 \pm 0.45$  Mn peaks per band pair (figure 3c) and  $5.70 \pm 0.83$  Mn peaks  $\text{yr}^{-1}$  (figure 3f). A comparison of upwelling indices and the approximately 1 month around release and recapture when location was known revealed species-specific relationships (figure 4). Corresponding linear relationships between upwelling intensity and vertebral Ba:Ca were significant for shortfin mako (figure 4a;  $y = 0.193x - 7.9$ ;  $F_{1,18} = 7.26$ ;  $p = 0.015$ ) and common thresher (figure 4b;  $y = 0.028x - 0.94$ ;  $F_{1,18} = 10.74$ ;  $p = 0.004$ ), but not blue shark (figure 4c).

### 4. Discussion

Reliable interpretation of elemental patterns in shark vertebrae to characterize life histories requires validation studies. Towards that end, this study compared vertebral elemental time-series among individuals from three species of sharks

from three different families, each with known age and known capture locations. We found evidence that Mn:Ca variation relates to band pair deposition and that Ba:Ca increases corresponds with the intensity of oceanic upwelling. These findings support the potential of Mn:Ca variation for estimating age and Ba:Ca concentrations, in some species, to reconstruct the relative intensity of upwelling in coastal and oceanic habitats, and more generally the potential of natural chemical tags for improving our understanding of population ecologies among elasmobranch species.

The uptake of trace elements in fish tissue and hard parts can occur via passage of dissolved ions from the water through the gill membrane or through diet and intestinal pathways; research to date suggests dietary uptake is dominant in elasmobranchs [39]. Metals in fish blood can occur as free hydrated species or may be bound in organic complexes or proteins [40], which can affect their incorporation into mineralized cartilage [38]. Alkaline earth metals (i.e. Mg, Ca, Sr, Ba) have similar ionic radii and +2 charge, which substitute for Ca during biomineralization of teleost otolith aragonite [41] and elasmobranch hydroxyapatite [21,38]. In precipitation of synthetic hydroxyapatite, Mn directly substitutes for Ca during formation [42]. Manganese concentrations have been found to be elevated in calcified tissues (vertebrae) compared to soft tissues in many species of shark, suggesting that Mn uptake and accumulation is related to calcium metabolism [43]. Although the pathway for Mn incorporation is not well understood, in shark vertebrae Mn variation appears to be coupled to band pair formation making it useful to age sharks.

#### (a) Manganese reflects age

The strong relationship between Mn and age corresponds to regular oscillations in Mn concentration in hypo- and hypermineralized band pairs. Hypomineralized regions associated with fast growth during spring and summer seasons have notably higher Mn concentrations. Several mechanisms could account for elevated Mn levels in hypomineralized zones of vertebra band pairs. If Mn is primarily from the diet, then periods of high prey consumption and rapid growth should result in more Mn incorporation. Alternatively, higher Mn in hypomineralized zones could be related to higher organic matter/protein content in vertebral tissue relative to the

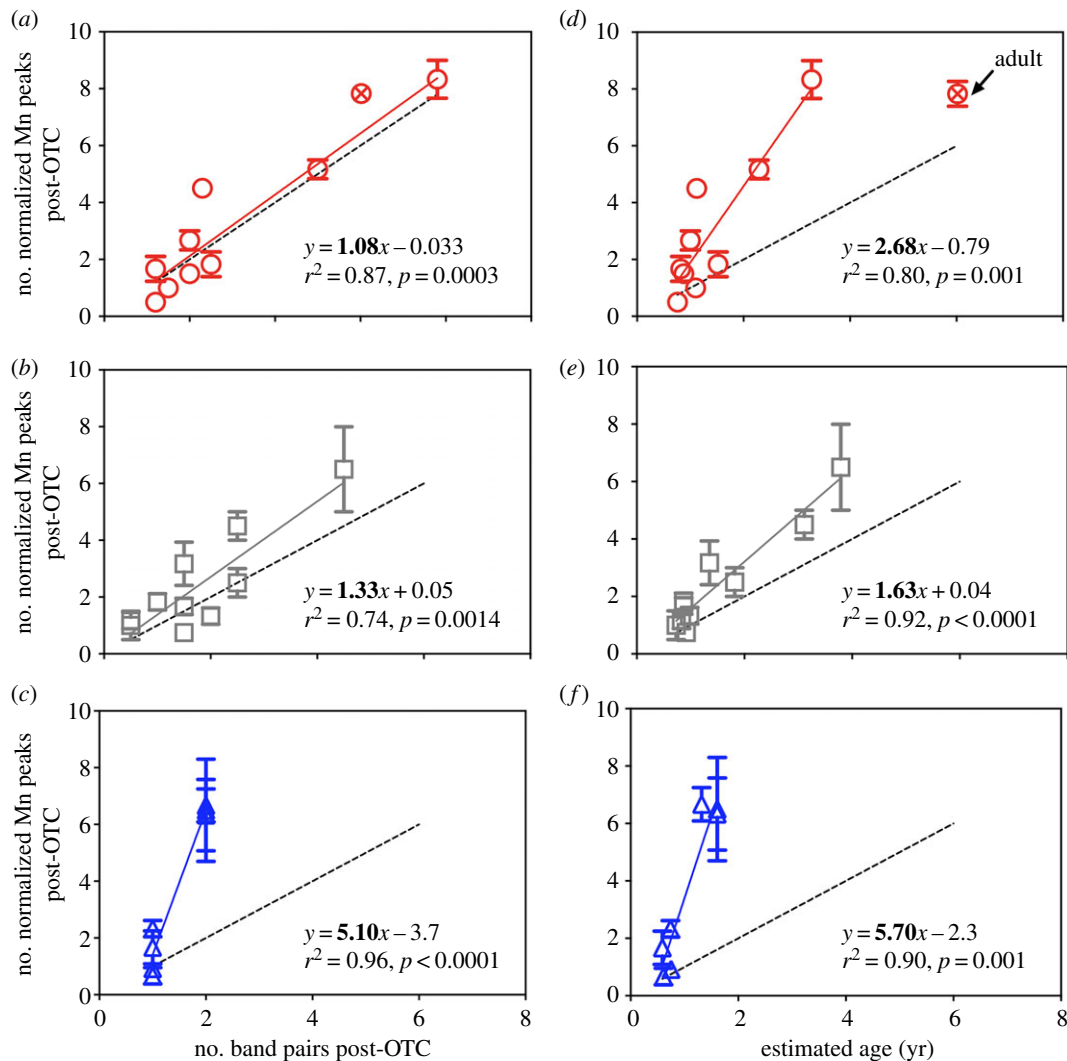


**Figure 3.** (a–c) Number of normalized Mn peaks post-OTC band versus number of band pairs post-OTC for (a) shortfin mako, (b) common thresher and (c) blue sharks. (d–f) Number of normalized Mn peaks post-OTC band versus validated age in years (yr) post-OTC band for (d) shortfin mako (e) common thresher and (f) blue sharks. Dashed black line = 1 : 1 relationship. The adult mako shark (circle with cross symbol) from [33] was not used in regression analysis. (Online version in colour.)

mineralized fraction during periods of faster growth [44]. It is plausible that Mn is incorporated into both the organic and inorganic fractions of vertebral cartilage, but at different proportions, as found in vertebrate bone [45]. All three species displayed different relationships between band pair deposition and Mn peaks. Common thresher displayed  $1.3 \pm 0.28$  Mn peak per band pair and about  $1.6 \pm 1.17$  Mn peak per year that corroborates annual band pair deposition [34,35,46]. The shortfin mako exhibited  $1.03 \pm 0.16$  Mn peak per band pair and  $2.68 \pm 0.5$  Mn peaks per year, which closely matches the bi-annual deposition rate in juveniles from both verification [47] and validation studies [28]. However, the single adult mako that was tagged at 5 years old, and then recaptured 6 years later did display 1.3 Mn peak per year, supporting annual band pair deposition in adult makos [33,48,49]. Blue sharks showed about five Mn peaks per band pair ( $5.1 \pm 0.45$ ) and per year ( $5.7 \pm 0.83$ ), but this species exhibited shorter times at liberty (0.6–1.6 yr) compared to the threshers and makos. Determining Mn peaks in blue sharks may have been hindered by shorter times at liberty and the challenges of identifying partial band pairs. Perhaps juvenile blue shark growth rates are variable within a season, resulting in multiple Mn peaks within a single band pair, because annual deposition has been previously validated in blue sharks [31].

Although Mn varied in a predictable manner with true age, the mechanisms driving variable Mn–age relationships among species require further study. Differences in Mn–age relationships could also be due to species-specific calcification physiology [50], dietary preferences [51], or migration patterns and habitat use [5]. For example, telemetry studies of blue sharks have found seasonally variable depth preferences, perhaps due to feeding upon seasonally abundant prey associated with different depths [52]. A comparative study of diets among these three species from the California coast reported opportunistic feeding and diverse diets in makos and blue sharks feeding primarily on squid and fish, but dietary specialization in thresher sharks preferring small schooling fish [51]. Additionally, males and females were not equally represented among the species in this study and had to be examined together due to limited sample sizes, which may have induced variability in terms of physiology and behaviour between sexes or size classes. Using elemental profiles obtained from vertebrae could potentially be used to estimate and validate age, derive age–length relationships and estimate growth rates based on large numbers of samples, if the species-specific relationship between band pair deposition and elemental chemistry are well characterized. Although vertebrae sampling is necessarily lethal, it does not require recapture of individuals

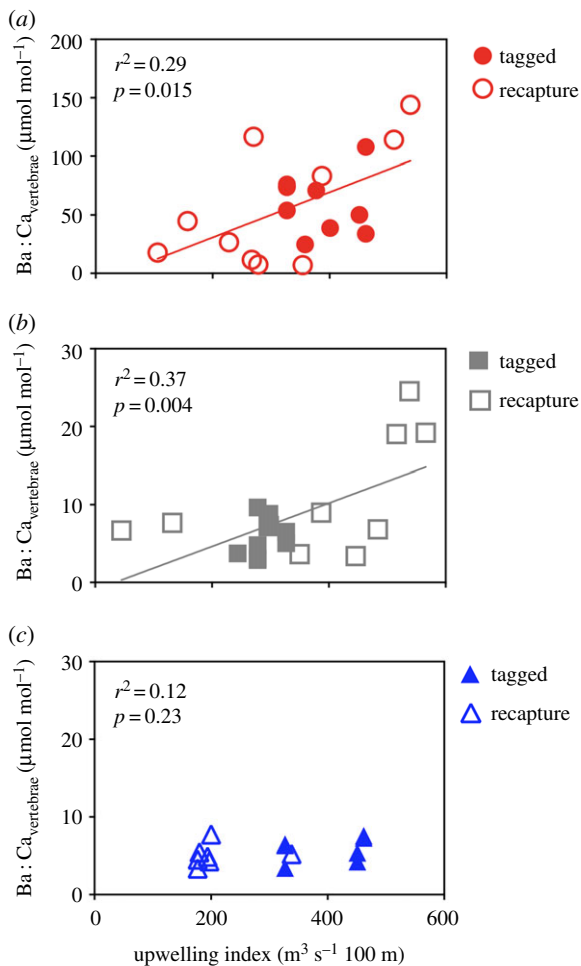


**Figure 4.** Relationship between cumulative monthly upwelling index (month of capture + previous month) at nearest station and Ba:Ca in vertebrae from known OTC tagging location (solid symbols) and known recapture location (open symbols) for (a) shortfin mako red circles, (b) common thresher (grey squares) and (c) blue shark (blue triangles). Solid coloured lines indicate linear regression equations. (Online version in colour.)

and could be applied to sharks that are difficult to tag and recapture, such as deep-sea species with limited life-history information [53]. Vertebral elemental analyses may offer an advantage over traditional age validation approaches, such as OTC tagging and recapture that are time consuming, expensive and limited by small sample sizes [1].

### (b) Barium reflects upwelling intensity

Oceanic upwelling transports deep, nutrient-rich (e.g. P, N, Si, Ba, Cd) cold water to the surface due to wind-driven Ekman transport [54]. Regions of upwelling exhibit increased Ba concentrations in surface waters [55], which may be incorporated in associated biominerals such as teleost fish otoliths [56] and coral skeletons [57,58]. That vertebral Ba levels over the approximately one month period examined in shortfin makos and common threshers correspond to the intensity of oceanic upwelling at known capture locations and dates along the California coast demonstrates the potential of shark vertebrae for proxying aspects of water mass chemistry. Barium patterns in the vertebrae of white sharks (*Carcharodon carcharias*) have been suggested to be derived from seasonal upwelling off South Africa [16].

Physiological controls of vertebral Ba variation in elasmobranchs are unknown with few controlled studies [21,22], but could be related to reduced sea surface temperature or

increased dissolved [Ba] in seawater, both associated with upwelling conditions. Smith *et al.* [21] found the temperature and ambient dissolved element concentrations can influence vertebral chemistry. Using round stingrays *Urolophus halleri* held for 3.6–8 months in three temperatures (16°, 18°, 24°) and three dissolved barium concentrations (1×, 3×, 6× ambient), they found a negative relationship between temperature and barium incorporation and a significant positive relationship between vertebrae and water Ba:Ca. Cold upwelled waters with higher Ba:Ca concentrations, may have likewise influenced Ba uptake in the shortfin mako and common thresher vertebrae studied here. Consistent with this result, synthetic hydroxyapatite incorporates more Ba at lower temperatures [59]. Alternatively, if vertebrae Ba concentration is also influenced by dietary pathways, then sharks feeding in upwelling regions may incorporate elevated levels of Ba from ingested prey [60]. Juvenile threshers use highly productive continental shelf waters as nursery habitat and display a preference for the upper mixed layer (less than 20 m) where there is abundant northern anchovy *Engraulis mordax* prey [30]. In the California Current region, anchovy populations become more abundant during high upwelling years [61].

Based on validated vertebral-based growth rates, a distance of 100 µm represents approximately one month of time. Previous studies reporting elemental uptake rates of two to four weeks for elasmobranch vertebrae chemistry to equilibrate with water chemistry [21,22]. Thus, the time frames represented by the vertebrae Ba:Ca sampling and upwelling index match temporally, which may contribute to the statistically significant relationship between upwelling and barium in shortfin makos and common threshers.

The lack of a significant relationship between vertebrae Ba:Ca and upwelling intensity for blue sharks could result from a range of factors. Blue shark diet, habitat and physiology differs from shortfin makos and thresher sharks. Blue sharks spend more time in pelagic oceanic habitats [62], have a greater reliance on deep water prey associated with the deep scattering layer (DSL) [51,52], and use offshore nursery habitats. In comparison, shortfin mako and thresher shark spend more time in coastal habitats and the nursery habitat for both species is considered to be the coastal waters, including the continental shelf and edge where upwelling occurs [29,30]. The diets of mako and thresher sharks include organisms of the DSL but to a lesser extent than blue sharks, and at smaller sizes mako and thresher sharks forage on a range of species. Additionally, being ectotherms, blue sharks probably have the lowest metabolic rates of the three species, whereas mako and thresher sharks are regionally endothermic and use a heat-exchanging circulatory system that maintains muscle temperature above ambient water temperature [63,64]. A lower metabolic rate may influence rates of uptake and incorporation of Ba:Ca. These differences in diet, habitat and metabolic rates among species, likely explain the discrepancy between vertebrae barium and upwelling in blue sharks compared to shortfin makos and common threshers.

## 5. Conclusion

Elemental patterns in mineralized vertebral cartilage from individuals of three shark species, each with known capture–recapture (liberty) durations and locations are interpreted as proxies of age (Mn:Ca) and intensity of environmental

upwelling (Ba:Ca). Patterns are species-specific, with differences likely related to varied habitats and thermal preferences (coastal upwelling zones versus pelagic habitat), metabolic rates (endothermic versus ectothermic) and foraging ecology. Only one sexually mature shortfin mako was analysed in this study and future work should include older sharks to characterize elemental chemistry across ontogeny and potential variations associated with reproduction and sexually dimorphic behaviour. Multi-decadal archives of shark vertebrae are available in historical collections that could be used to establish long-term climate biochronologies and investigate how oceanic regimes (e.g. El Niño, Pacific Decadal Oscillation) affect upwelling recorded in vertebral barium patterns and the consequences for growth, by measuring band-pair increment width (e.g. [65]). This information could be used to inform ecosystem-based management practices to better conserve predator populations.

## References

- Cailliet GM. 2015 Perspectives on elasmobranch life-history studies: A focus on age validation and relevance to fishery management. *J. Fish Biol.* **87**, 1271–1292. (doi:10.1111/jfb.12829)
- Smith SE, Au DW, Show C. 1998 Intrinsic rebound potentials of 26 species of Pacific sharks. *Mar. Freshw. Res.* **49**, 663–678. (doi:10.1071/MF97135)
- Chapman DD, Feldheim KA, Papastamatiou YP, Hueter RE. 2015 There and back again: a review of residency and return migrations in sharks, with implications for population structure and management. *Ann. Rev. Mar. Sci.* **7**, 547–570. (doi:10.1146/annurev-marine-010814-015730)
- Ellis JR, McCully Phillips SR, Poisson F. 2017 A review of capture and post-release mortality of elasmobranchs. *J. Fish Biol.* **90**, 653–722. (doi:10.1111/jfb.13197)
- Camhi MD, Pikitch EK, Babcock EA. 2008 *Sharks of the open ocean: biology, fisheries and conservation*. Oxford, UK: Blackwell Publishing.
- Harry AV. 2018 Evidence for systemic age underestimation in shark and ray ageing studies. *Fish Fish.* **19**, 185–200. (doi:10.1111/faf.12243)
- Dean MN, Ekstrom L, Monsonego-Ornan E, Ballantyne J, Witten PE, Riley C, Habraken W, Omelon S. 2015 Mineral homeostasis and regulation of mineralization processes in the skeletons of sharks, rays and relatives (Elasmobranchii). *Semin. Cell Dev. Biol.* **46**, 51–67. (doi:10.1016/j.semcdb.2015.10.022)
- Dean MN. 2011 *Cartilaginous fish skeletal tissues*. Amsterdam, The Netherlands: Elsevier.
- Ferreira BP, Vooren CM. 1991 Age, growth and structure of vertebra in the School Shark *Galeorhinus galeus* (Linnaeus 1758) from Southern Brazil. *Fish. Bull.* **89**, 19–32.
- Officer RA, Day RW, Clement JG, Brown LP. 1997 Captive gummy sharks, *Mustelus antarcticus*, form hypermineralised bands in their vertebrae during winter. *Can. J. Fish. Aquat. Sci.* **54**, 2677–2683. (doi:10.1139/cjfas-54-11-2677)
- Campana SE, Natanson LJ, Myklevoll S. 2002 Bomb dating and age determination of large pelagic sharks. *Can. J. Fish. Aquat. Sci.* **455**, 450–455. (doi:10.1139/F02-027)
- Clement JG. 1992 Reexamination of the fine-structure of endoskeletal mineralization in Chondrichthyan: implications for growth, aging and calcium homeostasis. *Aust. J. Mar. Freshw. Res.* **43**, 157–181. (doi:10.1071/MF9920157)
- Cailliet GM. 1990 Elasmobranch age determination and verification: an updated review. *Natl. Ocean. Atmos. Adm. Tech. Rep.* **90**, 157–165.
- Kerr L, Andrews A, Cailliet G, Brown T, Coale K. 2006 Investigations of  $\Delta^{14}\text{C}$ ,  $\delta^{13}\text{C}$ , and  $\delta^{15}\text{N}$  in vertebrae of white shark (*Carcharodon carcharias*) from the eastern North Pacific Ocean. *Environ. Biol. Fishes* **77**, 337–353. (doi:10.1007/S10641-006-9125-1)
- Hale LF, Dudgeon JV, Mason AZ, Lowe CG. 2006 Elemental signatures in the vertebral cartilage of the round stingray, *Urolophus halleri*, from Seal Beach, California. *Environ. Biol. Fishes* **77**, 317–325. (doi:10.1007/s10641-006-9124-2)
- Christiansen H. 2011 Developing and applying elemental composition of shark vertebrae as a tool for quantifying life history characteristics over ontogeny. MS thesis, University of Windsor, Ontario, Canada.
- Scharer RM, Patterson WF, Carlson JK, Poulakis GR. 2012 Age and growth of endangered smalltooth sawfish (*Pristis pectinata*) verified with LA-ICP-MS analysis of vertebrae. *PLoS ONE* **7**, e47850. (doi:10.1371/journal.pone.0047850)
- Jones BC, Geen GH. 1977 Age determination of an elasmobranch (*Squalus acanthias*) by X-ray spectrometry. *J. Fish. Res. Board Canada* **34**, 44–48. (doi:10.1139/f77-005)
- Cailliet G, Radtke R. 1987 A progress report on the electron microprobe analysis technique for age determination and verification in elasmobranchs. In *Age and growth of fish* (eds R Summerfelt, G Hall), pp. 359–369. Ames, IA: Iowa State University Press.
- Raoult V, Peddemors VM, Zahra D, Howell N, Howard DL, de Jonge MD, Williamson JE. 2016 Strontium mineralization of shark vertebrae. *Sci. Rep.* **6**, 29698. (doi:10.1038/srep29698)
- Smith WD, Miller JA, Heppell SS. 2013 Elemental markers in elasmobranchs: effects of environmental history and growth on vertebral chemistry. *PLoS ONE* **8**, e62423. (doi:10.1371/journal.pone.0062423)
- Werry JMA, Lee SYA, Otway NMC, Hu YD, Sumpton WE. 2011 A multi-faceted approach for quantifying the estuarine–nearshore transition in the life cycle of the bull shark, *Carcharhinus leucas*. *Mar. Freshw. Res.* **62**, 1421–1431. (doi:10.1071/MF11136)
- Tillett BJ, Meekan MG, Parry D, Munksgaard N, Field IC, Thorburn D, Bradshaw CJA. 2011 Decoding fingerprints: elemental composition of vertebrae correlates to age-related habitat use in two morphologically similar sharks. *Mar. Ecol. Prog. Ser.* **434**, 133–142. (doi:10.3354/meps09222)
- Smith WD, Miller JA, Marquez-Farias JF, Heppell SS. 2016 Elemental signatures reveal the geographic origins of a highly migratory shark: Prospects for measuring population connectivity. *Mar. Ecol. Prog. Ser.* **556**, 173–193. (doi:10.3354/meps11844)
- Izzo C, Huvneers C, Drew M, Bradshaw CJA, Donnellan SC, Gillanders BM. 2016 Vertebral chemistry demonstrates movement and population structure of bronze whaler. *Mar. Ecol. Prog. Ser.* **556**, 195–207. (doi:10.3354/meps11840)
- McMillan MN, Izzo C, Junge C, Albert OT, Jung A, Gillanders BM. 2016 Analysis of vertebral chemistry to assess stock structure in a deep-sea shark, *Etmopterus spinax*. *ICES J. Mar. Sci. J. du Cons.* **74**, fsw176. (doi:10.1093/icesjms/fsw176)
- Lewis JP, Patterson WF, Carlson JK, McLachlin K. 2016 Do vertebral chemical signatures distinguish juvenile blacktip shark (*Carcharhinus limbatus*) nursery regions in the northern Gulf of Mexico? *Mar. Freshw. Res.* **67**, 1014–1022. (doi:10.1071/MF15088)
- Wells RJD, Smith SE, Kohin S, Freund E, Spear N, Ramon DA. 2013 Age validation of juvenile Shortfin

**Data accessibility.** The dataset supporting this article is available in the electronic supplementary material.

**Authors' contributions.** J.A.M., R.J.D.W., S.Z.H. and O.S.C. designed the study. J.A.M. collected and analysed the data and wrote the manuscript. N.R.M. collected and analysed data. S.Z.H. and O.S.N. helped interpret the data. S.K., H.D., M.K., O.S. and R.J.D.W. provided samples and helped interpret data. All authors helped write and edit the manuscript and approved final publication.

**Competing interests.** We declare we have no competing interests.

**Funding.** Funding was provided by the Texas A&M University CONA-CYT Collaborative Research Grant Program (Project 2016–026).

**Acknowledgements.** We thank all fishers and researchers involved with tagging and returning of vertebrae from OTC tagged sharks. All research and associated sampling was carried out under the State of California Department of Fish and Wildlife permit no. SC-13886 issued to the National Oceanic and Atmospheric Administration Southwest Fisheries Science Center (NOAA SWFSC). Two anonymous reviewers helped improve this manuscript.

- Mako (*Isurus oxyrinchus*) tagged and marked with oxytetracycline off southern California. *Fish. Bull.* **111**, 147–160. (doi:10.7755/FB.111.2.3)
29. Sepulveda C, Kohin S, Chan C, Vetter R, Graham J. 2004 Movement patterns, depth preferences, and stomach temperatures of free-swimming juvenile mako sharks, *Isurus oxyrinchus*, in the Southern California Bight. *Mar. Biol.* **145**, 191–199. (doi:10.1007/s00227-004-1356-0)
  30. Cartamil D, Wegner N, Kacev D, Kohin S, Graham J. 2010 Movement patterns and nursery habitat of juvenile thresher sharks *Alopias vulpinus* in the Southern California Bight. *Mar. Ecol. Prog. Ser.* **404**, 249–258. (doi:10.3354/meps08495)
  31. Wells RJD, Spear N, Kohin S. 2017 Age validation of the blue shark (*Prionace glauca*) in the eastern Pacific Ocean. *Mar. Freshw. Res.* **68**, 1130. (doi:10.1071/MF16054)
  32. Nakano H, Stevens JD. 2008 The biology and ecology of the Blue shark, *Prionace glauca*. In *Sharks of the open ocean: biology, fisheries and conservation* (eds M Camhi, E Pikitch, E Babcock), pp. 140–151. Oxford, UK: Blackwell Publishing.
  33. Kinney MJ, Wells RJD, Kohin S. 2016 Oxytetracycline age validation of an adult shortfin mako shark *Isurus oxyrinchus* after 6 years at liberty. *J. Fish Biol.* **89**, 1828–1833. (doi:10.1111/jfb.13044)
  34. Spear N. 2017 Age validation of the common thresher shark (*Alopias vulpinus*) in the northeastern Pacific Ocean. MS thesis, Texas A&M University, Galveston, TX.
  35. Natanson LJ, Hamady LL, Gervelis BJ. 2015 Analysis of bomb radiocarbon data for common thresher sharks, *Alopias vulpinus*, in the northwestern Atlantic Ocean with revised growth curves. *Environ. Biol. Fishes* **99**, 39–47. (doi:10.1007/s10641-015-0452-y)
  36. Mohan JA, TinHan TC, Miller NR, David Wells RJ. 2017 Effects of sample cleaning and storage on the elemental composition of shark vertebrae. *Rapid Commun. Mass Spectrom.* **31**, 2073–2080. (doi:10.1002/rcm.7998)
  37. Hellstrom JC, Paton C, Woodhead JD, Hergt J. 2008 Lolite: software for spatially resolved LA-(quad and MC) ICPMS analysis. *Mineral. Assoc. Canada Short Course* **40**, 343–348.
  38. McMillan MN, Izzo C, Wade B, Gillanders BM. 2017 Elements and elasmobranchs: hypotheses, assumptions and limitations of elemental analysis. *J. Fish Biol.* **90**, 559–594. (doi:10.1111/jfb.13189)
  39. Mathews T, Fisher NS. 2009 Dominance of dietary intake of metals in marine elasmobranch and teleost fish. *Sci. Total Environ.* **407**, 5156–5161. (doi:10.1016/j.scitotenv.2009.06.003)
  40. Sturrock AM, Trueman CN, Darnaude AM, Hunter E. 2012 Can otolith elemental chemistry retrospectively track migrations in fully marine fishes? *J. Fish Biol.* **81**, 766–795. (doi:10.1111/j.1095-8649.2012.03372.x)
  41. Thomas ORB, Ganio K, Roberts BR, Swearer SE. 2017 Trace element–protein interactions in endolymph from the inner ear of fish: implications for environmental reconstructions using fish otolith chemistry. *Metalomics* **9**, 239–249. (doi:10.1039/C6MT00189K)
  42. Pon-On W, Meejoo S, Tang IM. 2008 Substitution of manganese and iron into hydroxyapatite: Core/shell nanoparticles. *Mater. Res. Bull.* **43**, 2137–2144. (doi:10.1016/j.materresbull.2007.09.004)
  43. Vas P. 1991 Trace metal levels in sharks from British and Atlantic waters. *Mar. Pollut. Bull.* **22**, 67–72. (doi:10.1016/0025-326X(91)90138-I)
  44. Melancon S, Fryer BJ, Gagnon JE, Ludsin SA. 2008 Mineralogical approaches to the study of biomineralization in fish otoliths. *Mineral. Mag.* **72**, 627–637. (doi:10.1180/minmag.2008.072.2.627)
  45. Fore H, Morton R. 1952 The manganese in bone. *Biochem. J.* **51**, 598–600. (doi:10.1042/bj0510598)
  46. Smith SE, Rasmussen RC, Ramon DA, Cailliet GM. 2008 The biology and ecology of thresher sharks (Alopiidae). In *Shark of the open ocean* (eds M Camhi, E Pikitch, E Babcock), pp. 60–68. Oxford, UK: Blackwell.
  47. Pratt H, Casey J. 1983 Age and growth of shortfin mako, *Isurus oxyrinchus*, using four methods. *Can. J. Fish. Aquat. Sci.* **40**, 1944–1957. (doi:10.1139/f83-224)
  48. Ardizzone D, Cailliet GM, Natanson LJ, Andrews AH, Kerr LA, Brown TA. 2006 Application of bomb radiocarbon chronologies to shortfin mako (*Isurus oxyrinchus*) age validation. *Environ. Biol. Fishes* **77**, 355–366. (doi:10.1007/s10641-006-9106-4)
  49. Natanson LJ, Kohler NE, Ardizzone D, Cailliet GM, Wintner SP, Mollet HF. 2006 Validated age and growth estimates for the shortfin mako, *Isurus oxyrinchus*, in the North Atlantic Ocean. *Environ. Biol. Fishes* **77**, 367–383. (doi:10.1007/s10641-006-9127-z)
  50. Porter ME, Beltran J, Koob T, Summers AP. 2006 Material properties and biochemical composition of mineralized vertebral cartilage in seven elasmobranch species (Chondrichthyes). *J. Exp. Biol.* **209**, 2920–2928. (doi:10.1242/jeb.02325)
  51. Preti A, Soykan CU, Dewar H, Wells RJD, Spear N. 2012 Comparative feeding ecology of shortfin mako, blue and thresher sharks in the California Current. *Environ. Biol. Fishes* **95**, 127–146. (doi:10.1007/s10641-012-9980-x)
  52. Carey FG, Scharold JV. 1990 Movements of blue sharks (*Prionace glauca*) in depth and course. *Mar. Biol.* **106**, 329–342. (doi:10.1007/BF01344309)
  53. García VB, Lucifora LO, Myers RA. 2008 The importance of habitat and life history to extinction risk in sharks, skates, rays and chimaeras. *Proc. R. Soc. B* **275**, 83–89. (doi:10.1098/rspb.2007.1295)
  54. Huyer A. 1983 Coastal upwelling in the California current system. *Prog. Oceanogr.* **12**, 259–284. (doi:10.1016/0079-6611(83)90010-1)
  55. Hsieh Y Te, Henderson GM. 2017 Barium stable isotopes in the global ocean: tracer of Ba inputs and utilization. *Earth Planet. Sci. Lett.* **473**, 269–278. (doi:10.1016/j.epsl.2017.06.024)
  56. Woodson LE, Wells BK, Grimes CB, Franks RP, Santora JA, Carr MH. 2013 Water and otolith chemistry identify exposure of juvenile rockfish to upwelled waters in an open coastal system. *Mar. Ecol. Prog. Ser.* **473**, 261–273. (doi:10.3354/meps10063)
  57. Gonnea ME, Cohen AL, DeCarlo TM, Charette MA. 2017 Relationship between water and aragonite barium concentrations in aquaria reared juvenile corals. *Geochim. Cosmochim. Acta* **209**, 123–134. (doi:10.1016/j.gca.2017.04.006)
  58. Lea DW, Shen GT, Boyle EA. 1989 Coralline barium records temporal variability in equatorial Pacific upwelling. *Nature* **340**, 373–376. (doi:10.1038/340373a0)
  59. Balter V, Lécuyer C. 2004 Determination of Sr and Ba partition coefficients between apatite and water from 5°C to 60°C: a potential new thermometer for aquatic paleoenvironments. *Geochim. Cosmochim. Acta* **68**, 423–432. (doi:10.1016/S0016-7037(00)00453-8)
  60. Woodcock SH, Grieshaber CA, Walther BD. 2012 Dietary transfer of enriched stable isotopes to mark otoliths, fin rays, and scales. *Can. J. Fish. Aquat. Sci.* **70**, 1–4. (doi:10.1139/cjfas-2012-0389)
  61. Allen LG, DeMartini EE. 1983 Temporal and spatial patterns of nearshore distribution and abundance of the pelagic fishes off San Onofre, Oceanside, California. *Fish. Bull.* **81**, 569–586.
  62. Nakano H, Seki MP. 2003 Synopsis of biological data on the blue shark, *Prionace glauca* Linnaeus. *Bull. Fish. Res. Agency* **6**, 18–55.
  63. Wolf NG, Swift PR, Carey FG. 1988 Swimming muscle helps warm the brain of lamnid sharks. *J. Comp. Physiol. B Biochem. Syst. Environ. Physiol.* **157**, 709–715. (doi:10.1007/BF00691001)
  64. Sepulveda CA, Graham JB, Bernal D. 2007 Aerobic metabolic rates of swimming juvenile mako sharks, *Isurus oxyrinchus*. *Mar. Biol.* **152**, 1087–1094. (doi:10.1007/s00227-007-0757-2)
  65. Black BA, Boehlert GW, Yoklavich MM. 2008 Establishing climate–growth relationships for yelloweye rockfish (*Sebastes ruberrimus*) in the northeast Pacific using a dendrochronological approach. *Fish. Oceanogr.* **17**, 368–379. (doi:10.1111/j.1365-2419.2008.00484.x)